THE ASTROPHYSICAL JOURNAL, 639:L51–L54, 2006 March 10

POWERFUL HIGH-VELOCITY DISPERSION MOLECULAR HYDROGEN ASSOCIATED WITH AN INTERGALACTIC SHOCK WAVE IN STEPHAN'S QUINTET

P. N. APPLETON,[1] KEVIN C. XU,[2] WILLIAM REACH,[1] MICHAEL A. DOPITA,[3] Y. GAO,[4] N. LU,[1] C. C. POPESCU,[5] J. W. SULENTIC,[6] R. J. TUFFS,[5] AND M. S. YUN[7]

Received 2005 October 10; accepted 2006 January 25; published 2006 February 13

ABSTRACT

We present the discovery of strong mid-infrared emission lines of molecular hydrogen of apparently high-velocity dispersion (~870 km s^{-1}) originating from a group-wide shock wave in Stephan's Quintet. These *Spitzer Space Telescope* observations reveal emission lines of molecular hydrogen and little else. This is the first time an almost pure H_2 line spectrum has been seen in an extragalactic object. Along with the absence of PAH-dust features and very low excitation ionized gas tracers, the spectra resemble shocked gas seen in Galactic supernova remnants, but on a vast scale. The molecular emission extends over 24 kpc along the X-ray–emitting shock front, but it has 10 times the surface luminosity as the soft X-rays and about one-third the surface luminosity of the IR continuum. We suggest that the powerful H_2 emission is generated by the shock wave caused when a high-velocity intruder galaxy collides with filaments of gas in the galaxy group. Our observations suggest a close connection between galaxy-scale shock waves and strong broad H_2 emission lines, like those seen in the spectra of ultraluminous infrared galaxies where high-speed collisions between galaxy disks are common.

Subject headings: galaxies: evolution — galaxies: individual (NGC 7318b) — galaxies: interactions — intergalactic medium

1. INTRODUCTION

Stephan's Quintet (hereafter SQ) is a system of four strongly interacting galaxies in a compact group and a likely foreground galaxy seen in projection against them (Allen 1970). One of the most remarkable aspects of SQ is an ~40 kpc long nonthermal radio continuum structure (see Fig. 1) lying in intergalactic space between the galaxies (Allen & Hartsuiker 1972; van der Hulst 1981). The same structure is also seen in X-rays and has been shown to be consistent with a large-scale shock wave, based on the optical spectroscopy (Pietsch et al. 1997; Trinchieri et al. 2005; Xu et al. 2003). It is probable (Sulentic et al. 2001) that the shock wave has formed because a high-velocity "intruder" galaxy, NGC 7318b, is colliding with the intergroup medium (IGM) located within the main group. We assume here a group distance of 94 Mpc, assuming a Hubble constant of 70 km s^{-1} Mpc^{-2} and a systemic velocity for the group as a whole of 6600 km s^{-1}.

2. OBSERVATIONS

We used the Infrared Spectrograph (IRS; Houck et al. 2004) on board the *Spitzer Space Telescope*[8] to take mid-IR spectra at the peak in the IR/radio emission from the shocked region. Observations were made on 2004 November 17 and December 8 using the Short-Low (SL), Short-High (SH), and Long-High (LH) modules of the spectrograph covering the wavelength ranges $\lambda = 5.3$–14.0, 10.0–19.5, and 18.8–37.2 μm, respectively. The raw data were processed through the SSC IRS S11-science pipeline to create two-dimensional flat-fielded images of the spectral orders. These data were further processed to remove the effects of the so-called rogue pixels that were not corrected by the pipeline. These pixels have erratic high dark currents that vary with time and were replaced using a simple pixel interpolation scheme. Flux and wavelength calibrations were performed using the standard calibration methods (Decin et al. 2004). Final extraction of the one-dimensional spectra was made using the SSC software SPICE, and line fluxes were measured using SMART (Higdon et al. 2004).

3. RESULTS

The top, middle, and bottom panels of Figure 2 show the spectra extracted in the region where all three slits overlap. Except for the atomic lines of [Ne II] 12.8 μm and [Si II] 34.8 μm, all are rotational transitions of the ground vibrational states of molecular hydrogen [the 0–0 $S(0)$, $S(1)$, $S(2)$, $S(3)$, and $S(5)$ lines]. To explore the excitation of the observed H_2 gas, we need to compare the line fluxes from the IRS slits that have different projected sizes on the sky, requiring that we make some assumptions about the spatial distribution of the molecules over the scale of the slits. From the SL slit oriented along the shock structure, we found that the H_2 emission was extended on the scale of 52″ (24 kpc), declining slowly from a small peak at the pointing center. We therefore consider three possible distributions: (1) H_2 originating in a point source (an unrealistic limiting case), (2) H_2 extended with constant surface brightness over the slits, and (3) a "preferred" case based on the observed SL distribution, assuming it has a similar spatial width to the radio emission. Table 1 provides a list of the lines and their measured fluxes, including upper limits for some key undetected lines.

Figure 3 shows the excitation diagram for H_2, (N/g) versus the upper-level energy, for the five detected hydrogen transitions and the one undetected hydrogen transition. N is the mo-

[1] *Spitzer* Science Center (SSC), California Institute of Technology, 1200 East California Boulevard, Pasadena, CA 91125; apple@ipac.caltech.edu.
[2] IPAC, California Institute of Technology, 1200 East California Boulevard, Pasadena, CA 91125.
[3] Research School of Astronomy and Astrophysics, Australian National University, Cotter Road, Weston Creek, ACT 2611, Australia.
[4] Purple Mountain Observatory, Chinese Academy of Sciences, 2 West Beijing Road, Nanjing 210008, China.
[5] Max-Planck-Institut für Kernphysik, Saupfercheckweg 1, 69117 Heidelberg, Germany.
[6] Department of Physics and Astronomy, University of Alabama, Tuscaloosa, AL 35487.
[7] Department of Astronomy, University of Massachusetts, Amherst, MA 01002.
[8] This work is based on observations made with the *Spitzer Space Telescope*, which is operated by the Jet Propulsion Laboratory, California Institute of Technology, under NASA contract 1407.

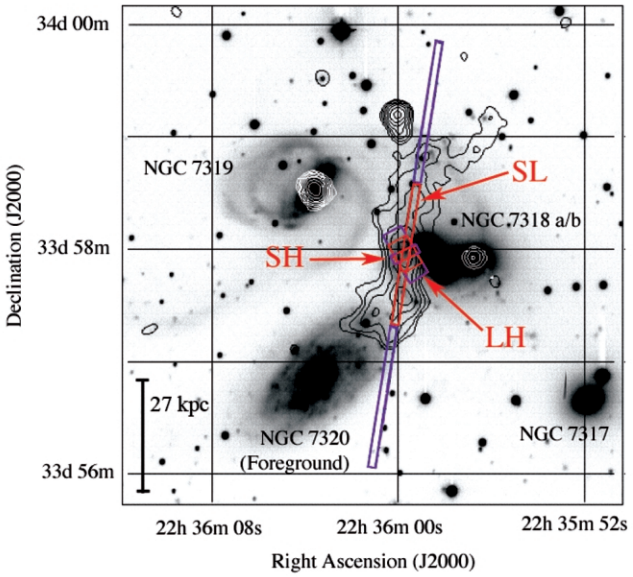

FIG. 1.—SQ showing the positioning of the IRS slits centered on α(J2000) = 22^{h}35^{m}59.57, δ(J2000) = +33°58′1.″8. Contours are VLA 1.4 GHz radio emission superposed on an *R*-band optical image (Xu et al. 2003). The X-ray emission (not shown here) follows closely that of the radio. Only the central portion of the slits (*red boxes*) were common to the two separate observing (nod) positions made in each IRS module slit (the purple shows the full coverage). SL = 57 × 3.6 arcsec^2, SH = 11.3 × 4.7 arcsec^2, and LH = 22.3 × 11.1 arcsecs^2. The scale bar assumes a distance to the group of 94 Mpc.

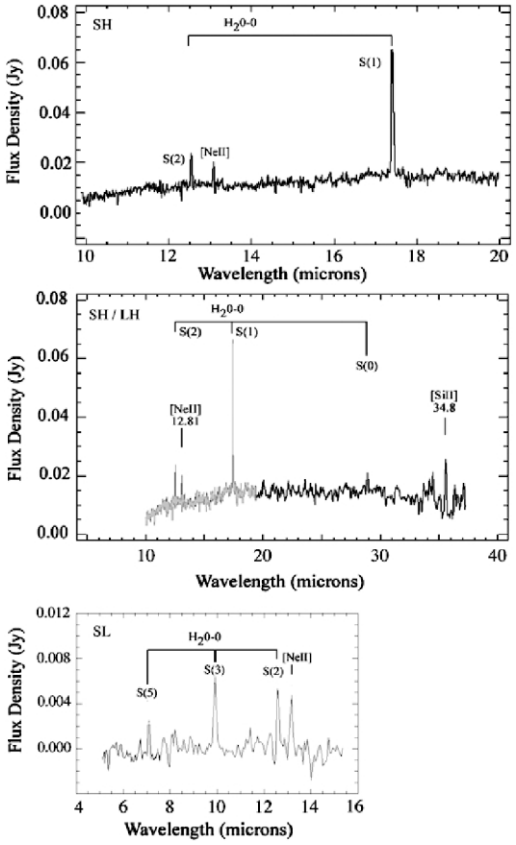

FIG. 2.—*Top*: IRS SH spectrum of the brightest radio/IR point in the shock front. *Middle*: Combined SH (*gray line*) and LH (*black line*) spectrum of the same target region assuming that the continuum can be used to match the two spectra at 20 μm. *Bottom*: SL spectrum at the same position. SL2 is the gray line, and SL1 is the black line. Note that there is no evidence of PAH emission.

lecular column density, and g is the statistical weight for that transition. The nonlinear decline of log (N/g) with upper-level energy is commonly seen in shocks within the Galaxy, as well as in external galaxies (Lutz et al. 2003; Rigopoulou et al. 2002), and is an indication that no single-temperature LTE model fits these data. There are no obvious deviations from the assumed ortho/para ratio = 3 visible in these plots. We fit a multitemperature model through the preferred data points, constraining the warm gas by the $S(0)/S(2)$ [para] ratio and allowing the higher order $S(3)/S(5)$ [ortho] transitions to provide a very rough guide to the temperature of a hotter component. Our data are consistent with a warm $T = 185 \pm 30$ K component (H_2 column density 2.06 × 10^{20} cm^{-2}) and $T = 675 \pm 80$ K (column 1.54 × 10^{18} cm^{-2}) for the hotter components. The choice of a two-component temperature model (especially the hotter component) is quite arbitrary: in reality (if our interpretation is correct that the emission arises in a highly turbulent medium), it is likely to be the sum of a continuous distribution of multitemperature components. However, the coolest component dominates the hydrogen column density estimates given here. We note that a multiphase medium could also lead to a similar excitation pattern.

The total H_2 line luminosity, accounting for an extra 40% in undetected lines, is 8.4 × 10^{40} ergs s^{-1} from the SH slit area alone. The corresponding H_2 mass in these warm/hot components seen in the SH slit is 3.4 × 10^7 $M_\odot$ ($\Sigma_{H_2} = 3.1$ $M_\odot$ pc^{-2}). The H_2 surface luminosity of 2.0 $L_\odot$ pc^{-2} is only a factor of 3 less than the IR continuum surface luminosity of 5.4 $L_\odot$ pc^{-2} (=2.5 × 10^{41} ergs s^{-1}) based on an extrapolation from unpub-

TABLE 1
LINE FLUXES SCALED TO THE EQUIVALENT SH-SLIT APERTURE

SPECTRAL FEATURE	IRS MODULE	FLUX[a] (10^{-22} W cm^{-2})		
		Uniform	Point-Source Limit	Preferred
H_2 0–0 $S(0)$	LH	1.9 ± 0.5	12.6 ± 3.3	4.2 ± 1.1
H_2 0–0 $S(1)$	SH	19.80 ± 0.57	19.80 ± 0.57	19.80 ± 0.57
H_2 0–0 $S(2)$	SH	6.41 ± 0.58	6.41 ± 0.58	6.41 ± 0.58
H_2 0–0 $S(3)$	SL	15.6 ± 1.1	8.1 ± 1.1	15.6 ± 1.1
H_2 0–0 $S(4)$	SL	<3.4 ± 1.1	<1.8 ± 1.1	<3.4 ± 1.1
H_2 0–0 $S(5)$	SL	7.8 ± 2.4	4.1 ± 2.4	7.8 ± 2.4
[Ne II] 12.81 μm	SH	3.49 ± 0.64	3.49 ± 0.64	3.49 ± 0.64
[Ne III] 15.55 μm	SH	<1.5 ± 0.64[b]	<1.5 ± 0.64[b]	<1.5 ± 0.64[b]
H_3^+ 16.33 μm	SH	<1.5 ± 0.64	<1.5 ± 0.64	<1.5 ± 0.64
[Si II] 34.8 μm	LH	3.5 ± 0.9	23.7 ± 5.7	7.9 ± 1.9

[a] Assumed distribution over the scale of the LH module (see text).
[b] Line may be marginally detected.

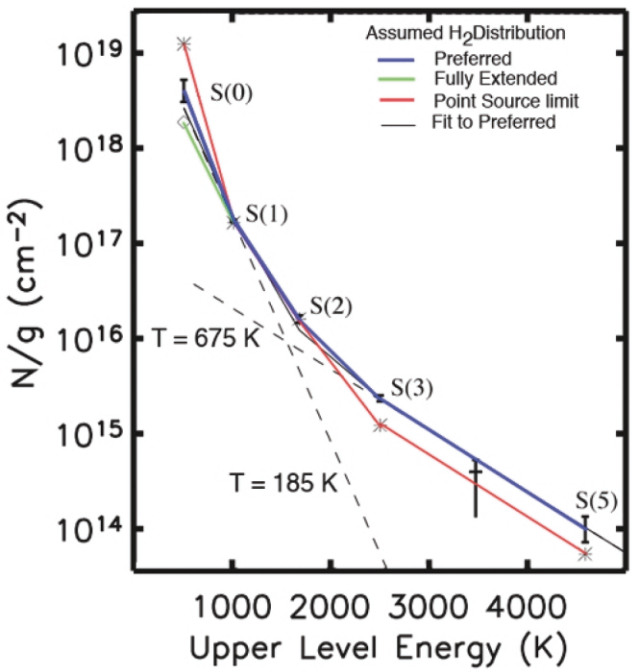

FIG. 3.—Excitation diagram for H_2. The colored lines represent three different assumed spatial distributions of the H_2 across the LH and SH slits. For SL, we scale the spectrum to that of SH using the 0–0 *S*(2) line that is detected in common. The blue line (and error bars) represents the preferred distribution based on an extrapolation from the H_2 distribution seen in the SL slit (see text); the green line and the red line show the limiting cases of an infinite distribution and a point-source distribution, respectively. The dotted lines represent a rough model for the preferred distribution that assumes a two-temperature fit to the points. The solid line represents the sum of these components.

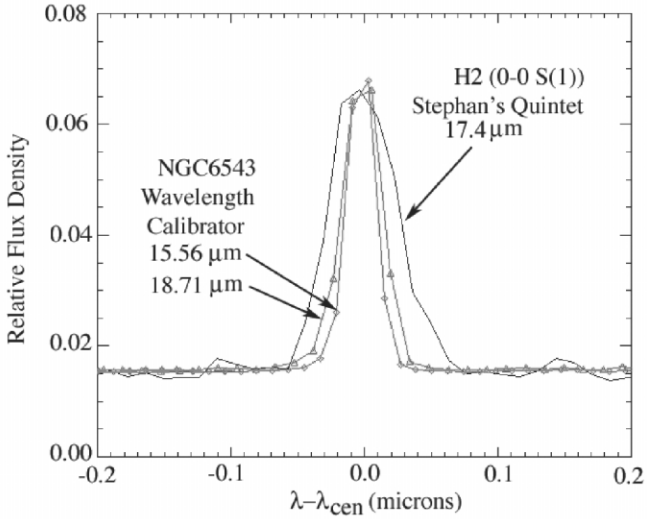

FIG. 4.—The 0–0 *S*(1) 17.0 μm molecular hydrogen line (detected with a signal-to-noise ratio of 33) is clearly resolved (intrinsic FWHM = 870 ± 60 km s^{-1}) by the IRS (*black line*) as compared with two unresolved spectral lines (R = 600) in the planetary nebula NGC 6543 at 15.6 and 18.7 μm that bracket the H_2 line (*gray line*). Similar broad widths are found for the 0–0 *S*(0) and 0–0 *S*(2) lines. The width of the [Ne II] 12.8 μm line is significantly less broad (intrinsic FWHM = 600 ± 80 km s^{-1}); the wavelength of the line center, λ_{cen}, is shown for the three lines in order to allow their widths to be compared.

lished 70 μm *Spitzer* data by one of us (R. J. T., and consistent with earlier *ISO* data from Xu et al. 2003). The corresponding H_2 lines and far-infrared (FIR) continuum surface brightnesses are 10 and 26 times the X-ray (0.5–1.5 keV) surface brightness (0.21 $L_\odot$ pc^{-2}), respectively. The dominance of the FIR continuum emission over the X-ray emission confirms that the shocked gas is cooling primarily through inelastic collisions of the ions and electrons with grains, as proposed by Xu et al. (2003, who derived a cooling timescale of ~2 Myr), and may explain the unexpectedly cool postshock X-ray gas seen in recent *XMM* observations (Trinchieri et al. 2005). However, the fact that a substantial minority of the total cooling also proceeds through H_2 lines comes as a surprise.

A remarkable feature of the *Spitzer* observations (Fig. 4) is the discovery that the H_2 line is extremely broad and resolved spectrally, even with the relative low resolution of the IRS (R = 600). Assuming a Gaussian decomposition from the instrument profile, we estimate the intrinsic width of the 0–0 *S*(1) line to be 870 ± 60 km s^{-1}, exceeding the largest known H_2 line width known to date (e.g., the ULIRG NGC 6240; $\Delta V \sim 680$ km s^{-1}; Lutz et al. 2003; Armus et al. 2006). Because H_2 is a fragile molecule that can easily be destroyed in 50 km s^{-1} J-type shocks (Hollenbach & McKee 1980, 1989), such a wide, potentially intrinsic, spread in molecular cloud velocities is extremely unusual.

The line width is comparable to the collision velocity ($\Delta V \sim$ 500–600 km s^{-1}) of NGC 7318b with either NGC 7319 or an intergalactic gas filament (Allen & Hartsuiker 1972; van der Hulst 1981; Williams et al. 2002; Sulentic et al. 2001; Trinchieri et al. 2003, 2005), suggesting that the H_2 emission is intimately linked to the formation of the radio and X-ray shock structure.

Although the IRS does not have the spectral resolution to determine whether the apparently broad line is made up of a number of narrow-line components blended together along the line of sight or whether the line is truly broad, there are some pieces of evidence that favor the latter. These are as follows: (1) Broad (ΔV = 1000 km s^{-1}) optical [O I] λ6300 line emission with excitation properties of shocked gas is seen at our observing position (Xu et al. 2003), whereas at other positions much farther from the peak of the X-ray/IR ridge narrower lines are seen. (2) Extremely high speed shocks are highly dissociative, and it is unlikely that preexisting H_2 or even more fragile polycyclic aromatic hydrocarbon (PAH) molecules could survive a >500 km s^{-1} collision with the intruder (Hollenbach & McKee 1980, 1989). Furthermore, the H_2 line luminosity that we see from the region (~2 $L_\odot$ pc^{-2}) is a significant fraction of the predicted (Dopita & Sutherland 1995, 1996) mechanical luminosity density in the shock (160 times the Hα surface density, $\sigma_{H\alpha} = 160 \times 0.13\ L_\odot$ pc^{-2} = 21 $L_\odot$ pc^{-2}). There would appear to be plenty of mechanical luminosity available to excite the H_2 molecules if they reformed in postshocked gas.

If we assume that a 500 km s^{-1} shock is driven into the IGM and that a second similar shock is driven into the intruder (assuming their densities are similar), this will create an unstable turbulent ($\Delta V \sim 1000$ km s^{-1}) cooling layer where the flows mix. If the gas can cool quickly enough, H_2 recombination would occur in that layer, and this would have the necessary properties to explain our observations, including the high-velocity dispersion from turbulence. The cooling timescale (Dopita & Sutherland 2003, p. 201) for the hot X-ray gas in each shock wave is τ_{cool}(Myr) = $0.24(V_{500})^{4.4}/Zn$, where V_{500} is the speed of the shock in units of 500 km s^{-1}, Z is the metallicity in solar units, and n is the preshock density (we assume n = 0.027 cm^{-3}, from X-ray observations; Trinchieri et al. 2003). For $V_{500} \sim 1$ and Z = 1, the cooling timescale τ_{cool} = 9.5 Myr, during which time the shock wave would have traveled ~5 kpc = 10″ (or twice this for the double shock). In reality, the cooling layer would be much sharper, since this analysis excludes the effects of IR cooling by dust, which is known to be very significant (Xu et al. 2003). This argument demonstrates that the postshocked gas

layer would cool fast enough to begin forming H_2 within the viewing zone of the IRS slits even for a mainly transverse geometry for the shock propagation as projected on the sky. The observed H_2 column of the cooler component ($\sim 2 \times 10^{20}$ cm^{-3}) could easily be built up over a scale of a few kiloparsecs from the available preshocked gas mass once the temperature of the gas had cooled sufficiently for H_2 to form.

One challenge for the postshock origin of the H_2 is to avoid putting too much of the shock dissipation energy into the X-ray component. Usually in high-speed shocks, X-ray dissipation dominates the cooling in the $T = 10^6$–10^4 K regime, before H_2 molecules can form, which is not the case here since H_2 line emission exceeds the X-rays by a factor of 10. Part of the answer may come from the even stronger IR continuum seen at longer wavelengths (Xu et al. 2003). Xu et al. argued that the principal coolant in the shock is from large grains that efficiently cool the shock through FIR emission. The H_2 emission from the postshocked material could be additionally boosted relative to the X-rays by invoking a glancing collision between the intruder galaxy and the IGM, which would create an oblique-shock geometry rather than a plane-parallel one. In oblique shocks, much more energy is carried in bulk transverse motions (hence reducing X-ray dissipation), and the shock is significantly weakened (e.g., Dopita & Sutherland 2003), while still allowing a fraction of the mechanical energy to cascade down to smaller and smaller scales (as in the Galactic interstellar medium [ISM]; e.g., McKee et al. 1984; Elmegreen & Scalo 2004), where shock speeds would be lower and where molecules could re-form in the postshocked medium. To test these ideas will require detailed three-dimensional hydrodynamic models beyond the scope of this observational Letter.

An alternative explanation for the H_2 emission is to postulate that the emission comes from a 500 km s^{-1} shock overrunning a clumpy preshocked medium. This has the advantage that dense clouds (embedded in a more diffuse medium) will experience much slower shocks and are more likely to cool through line emission than X-rays, whereas the FIR emission could come from grains emitting over the entire diffuse medium, thus partly explaining the anomalous H_2 line–to–IR continuum ratio. The large velocity dispersion could arise because the shock would eventually accelerate clouds to different velocities within the shock or because of multiple velocity components being present in the preshocked gas. The problem with this picture is that we might expect to see PAH emission from the precursor ISM, but this has not happened. We note that if the Hα emission seen from the shocked regions was scaled to an equivalent PAH line strength typical of those seen in the largest of the M51 H II regions (Calzetti et al. 2005), we should have easily (>10 σ) detected the signal, even in the case of no extinction correction for the Hα. Of course, the ISM of any precursor material is likely to contribute only a small factor to the Hα emission observed, but this provides an upper limit. The shock is also likely to be radiative, which could also help to destroy PAH molecules, whereas the more refractory grains must have been able to survive the shock. This model still has to be capable of predicting the large ratio of H_2 line luminosity relative to the IR continuum luminosity, implying that a lot of energy has to be somehow channeled into mechanical energy. Further modeling of these scenarios will be required in order to determine whether it can explain all the available data on the shock.

Future H_2 observations with much higher velocity and spatial resolution may allow us to explore further the nature of the emission mechanism that is generating such large H_2 line flux. There are hints of large-scale clumpiness in the H_2 distribution as seen by SL along the shock front, and studying the velocity and spatial inhomogeneities within the shock would be highly beneficial.

4. IMPLICATIONS FOR ULIRGs

The discovery of strong, high-velocity dispersion H_2 emission in a large-scale group-wide shock wave provides us with support for the idea (Rieke et al. 1985) that shock waves are primarily responsible for the strong H_2 emission lines seen in many ultraluminous infrared galaxies (ULIRGs). Indeed, our observations suggest $L(H_2) > 10^{41}$ ergs s^{-1} over the whole shock structure, comparable to the H_2 luminosity of Arp 220 but a factor of 10 less than NGC 6240 (Armus et al. 2006). An alternative idea for NGC 6240 is that X-rays heating the gas, rather than shocks, is the dominant mechanism for the IR lines in ULIRGs (Draine & Woods 1990). However, in addition to the low X-ray surface density compared with the H_2 lines, our spectra of SQ show little evidence of the H_3^+ 16.33 μm line, which is a key diagnostic of this model. Although the geometry of the shocks is unlikely to be identical to that suggested by the SQ observations, there is little doubt that large-scale shocks must be present in ULIRGs, where high-velocity streams of molecular gas must collide, especially in the early stages of a merger.

The authors thank A. Noriega-Crespo, L. Armus, D. Shupe, J. Ingalls, G. Helou (SSC), V. Charmandaris (University of Crete), and J. Houck (Cornell University) for comments and the referee, D. Hollenbach, for valuable suggestions.

Facilities: Spitzer

REFERENCES

Allen, R. J. 1970, A&A, 7, 330
Allen, R. J., & Hartsuiker, J. W. 1972, Nature, 239, 324
Armus, L., et al. 2006, ApJ, in press
Calzetti, D., et al. 2005, ApJ, 633, 871
Decin, L., Morris, P. W., Appleton, P. N., Charmandaris, V., & Houck, J. R. 2004, ApJS, 154, 408
Dopita, M. A., & Sutherland, R. S. 1995, ApJ, 455, 468
———. 1996, ApJS, 102, 161
———. 2003, Astrophysics of the Diffuse Universe (Berlin: Springer)
Draine, B. T., & Woods, D. T. 1990, ApJ, 363, 464
Elmegreen, B. G., & Scalo, J. 2004, ARA&A, 42, 211
Higdon, J. L., et al. 2004, PASP, 116, 975
Hollenbach, D., & McKee, C. F. 1980, ApJ, 241, L47
———. 1989, ApJ, 342, 306
Houck, J. R., et al. 2004, ApJS, 154, 18
Lutz, D., Sturm, E., Genzel, R., Spoon, H. W. W., Moorwood, A. F. M., Netzer, H., & Sternberg, A. 2003, A&A, 409, 867
McKee, C. F., Chernoff, D. F., & Hollenbach, D. J. 1984, in Proc. 16th ESLAB Symp., Galactic and Extragalactic Infrared Spectroscopy, ed. M. F. Kessler & J. P. Phillips (Dordrecht: Reidel), 103
Pietsch, W., Trinchieri, G., Arp, H., & Sulentic, J. W. 1997, A&A, 322, 89
Rieke, G. H., Cutri, R. M., Black, J. H., Kailey, W. F., McAlaray, C. W., Lebofsky, M. J., & Elston, R. 1985, ApJ, 290, 116
Rigopoulou, D., Kunze, D., Lutz., D., Genzel, R., & Moorwood, A. F. M. 2002, A&A, 389, 374
Sulentic, J. W., Rosado, M., Dultzin-Hacyan, D., Verdes-Montenegro, L., Trinchieri, G., Xu, C., & Pietsch, W. 2001, AJ, 122, 2993
Trinchieri, G., Sulentic, J., Breitschwerdt, D., & Pietsch, W. 2003, A&A, 401, 173
Trinchieri, G., Sulentic, J., Pietsch, W., & Breitschwerdt, D. 2005, A&A, 444, 697
van der Hulst, J. M., & Rots, A. H. 1981, AJ, 86, 1175
Williams, B. A., Yun, M. S., & Verdes-Montenegro, L. 2002, AJ, 123, 2417
Xu, K., Lu, N., Condon, J. J., Dopita, M., & Tuffs, R. J. 2003, ApJ, 595, 665